Manuscript submitted to *bioRxiv*

Article

Novel gramicidin-derived β-helical antimicrobial peptides

Edward Lambden[1,*] and Martin B. Ulmschneider[1]

[1]Department of Chemistry, King's College London, London
[*]Correspondence: edward.lambden@kcl.ac.uk

ABSTRACT Combating the threat of multidrug resistance bacteria requires many different approaches. Using structural motifs and sequences from existing antibacterial compounds affords a fresh attack against such bacteria, while circumventing inherited resistance against the existing compound. Gramicidin is a 16 amino acid peptide with an alternating L- and D- motif with highly bacteriocidal effects in gram-positive membranes. In the membrane it assumes a β-helix form with two peptides aligned by their N-terminal interactions, and only conducts in such a form. Using gramicidin as a basis, this study employs molecular dynamics simulations as an initial design step and evaluates gramicidin-derived candidates based on their backbone hydrogen-bond interactions, capacity for conductance, profile of their RMSD over the course of the simulation, and how the peptide interacts with the phospholipid headgroups. There are twelve candidate systems with results comparable to gramicidin and the factors at play in their efficacy are examined.

1 INTRODUCTION

β-helices have been a subject of scientific interest for much of the last century, as is the case for the linear peptide gramicidin (1), a family whose antibacterial properties have been known and investigated since the 1940s (2) (3). It is expressed in the soil bacteria *Bacillus brevis*, with its name derived from its bactericidal effects against Gram-positive bacteria. Gramicidins have a hydrophobic amino acid sequence of: Formyl-X1GAlAvVvX2lWlWlWG-ol (L-amino acids given in upper case and D-amino acids are given in lower case). (4). Ethanolamine is a glycine with a carbonyl oxygen. In gramicidin A, B, and C respectively, the X1 is VAL, VAL or ILE, and X2 is TRP, PHE, or TYR. The alternating L- and D- amino acids are crucial for the peptide to assume a β-helical form. This L- and D- alternating motif is unusual for naturally occurring peptides (5); gramicidin is synthesized by non-ribosomal multienzyme complexes, and the conversion of L - to D - amino acids takes place during the biosynthesis. At 16 residues, the sequence is too short to span the full hydrophobic lipid bilayer, however upon assumption of a helical dimer within the bilayer, conductance of monovalent cations occurs within the dimerised channel (6). Conductance occurs only when the N-termini of both of the dimers are linked via a hydrogen bond and stabilised within the membrane environment (7). The involvement of the N-termini in dimerisation was investigated through comparing the effect of C-terminal and N-terminal charged analogues (5). N-terminal charged analogues did not form conducting channels within black lipid membranes, which are model membranes developed in the 1960s, which are favoured for their ability to reconstitute proteins into the bilayer (8). Conversely, C-terminal charged analogues did produce conducting channels in these black lipid membrane environments. Gramicidin's selectivity for monovalent cations (9) lead to gramicidin being a popular choice to study ion channels within lipid bilayers.

The helical dimer forms a cylindrical tube with twelve parallel β-sheet-like hydrogen bonds between residues in adjacent turn, which provide stability to each of the monomers (10). The hydrophobicity and structure of amino acid residues contribute further to the stability, with TRP at the membrane-

solvent interface, and ALA and VAL buried more deeply. The abundance of TRP at the lipid-water interface and its abundance in membrane proteins suggests it plays an important anchoring role, with its favoured location driven by hydrogen-bonding between the indole N-H hydrogen and the carbonyl and phosphate oxygens (11). The gramicidin pore is $\approx 4-5$ Å in diameter with a length of 26 Å and 6.4 amino acid residues per turn (12) (13), and typically does not have side on contact between adjacent helices (13). Outside of a lipid membrane environment, a pair of gramicidin peptides energetically favour a double stranded helix form (14) - such a structure is non conducting in a bilayer.

The β-helix structure is diverse in nature - they can contain several β-strand regions linked by turns (15), or follow the helical dimer motif that gramicidin is known for. Gramicidin's propensity to form an ion channel for monovalent cations means its structure and sequence are powerful tools for the design of antimicrobial agents in the fight against multi-drug resistant bacteria. Gramicidin A's potency as a disruptive ion channel to begin the process of apoptosis has seen its possibility as an anticancer agent explored (16).

A selection of peptides are discussed here, with the effects of different amino acid compositions and sequence lengths on the stability and flux of these peptides considered. Gramicidin dimer channels, in a concentration of 0.1 M NaCl with 100mV applied across the membrane, have a conductance of a is $5.8 \cdot 10^{-12}\ \Omega^{-1}$ at 20°C (7). This is a benchmark for which the systems explored in this investigation will compared to. Several different residues per turn values were tested in the preliminary investigation before settling upon the explored value of 6.7, slightly higher than gramicidin's reported 6.4 residues per turn (17).

There are several design criteria that must be taken into account when designing a gramicidin-like peptide: (a) it must take on the form of a β-helix, which requires alternating L- and D- amino acids along its sequence, with h-bond interactions between the C=O and N-H groups driving the stability and structure of the peptide; (b) the core of the β-helix must be highly hydrophobic, possibly with stabilising tryptophans at either end of each sequence; (c) it must permit the passage of water and ions through the membrane. As with any design, it is pertinent to only introduce complexity once the fundamentals are understood. It is therefore that the sequences studied here are pure β-helical structures and will not contain loops, turns or α-helical sections as can often be found in β-helical proteins (18) (19) (20).

2 MATERIALS AND METHODS

2.1 Molecular dynamics simulation procedure

Unbiased molecular dynamics simulations were performed using the Charmm-36m forcefield (21) and Gromacs 2020.4 (22) (23). The membrane was composed of POPG and PVCL2 lipids in a 50:50 weight ratio (corresponding to a 1.8:1 numerical ratio) to mimic the membrane of *streptococcus pneumoniae* (24). Electrostatic interactions were computed using the particle mesh Ewald method (25), and a cutoff of 16 Å was used for the van der Waals interactions. The system was equilibrated in four stages with different time steps (0.1 fs, 0.5 fs, 1 fs, 2 fs), with the first two stages utilising an NVT ensemble, whilst the production runs were performed in an NPT ensemble with a 2 fs time step. Each system had a total equilibration time of 50 ns and a total production run of $1\mu s$. During the equilibration, a Berendsen thermostat (26) at 310K was employed. Neighbour lists were updated every ten steps. In the production runs, the solvent, lipids, and protein were separately coupled to a heat bath at a temperuate of 310K with a time constant $\tau = 0.1ps$ using the Nosé-Hoover thermostat (27). Atmospheric pressure of 1 bar was maintained using the Parrinello-Rahman barostat (28) with isotropic pressure coupling with compressibility $\kappa = 5 \cdot 10^{-5}$ bar^{-1} and a time constant $\tau = 1\ ps$. Analysis was performed using Python3.7, VMD (29), MDAnalysis (30), LiPyphilic (31), and PyMol (32).

2.2 Molecular dynamics preparation

The β-helix design began from measuring the ψ and ϕ angles of an experimentally resolved structure of gramicidin A (pdb: 1GRM) (33), using VMD. These values were averaged and used as a template for the initial structures. Using

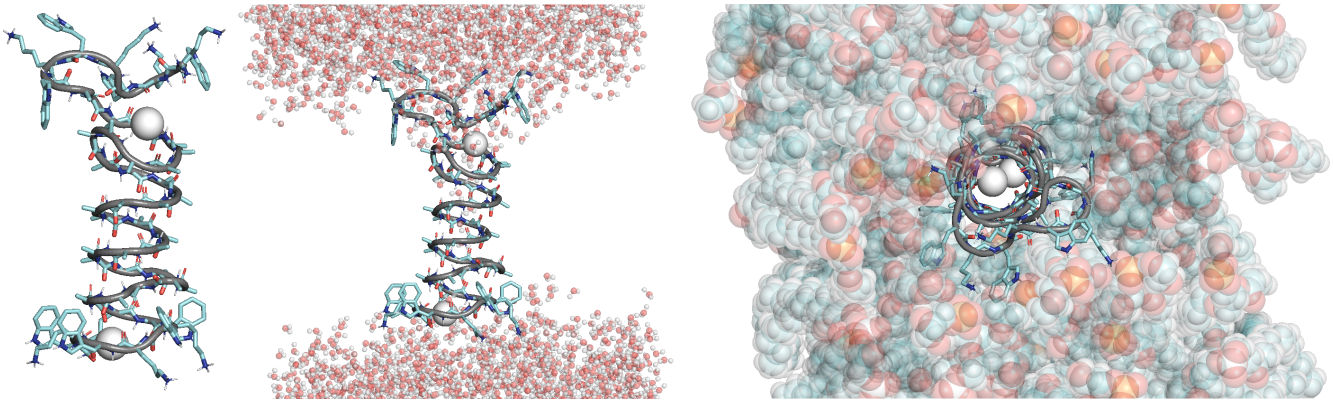

Figure 1: The 48-ALA-TRP system in three different views. Carbons are shown in cyan, nitrogens in blue, oxygens in red, and polar hydrogens in white, all as a ball and stick representation. The K+ ions are shown as white beads. The helical backbone is highlighted in grey, and K+ **Left:** Side on, with membrane and waters hidden and two K+ ions shown in the pore. **Middle:** Side on, with waters shown. **Right:** Top down, with waters hidden and the membrane shown, with phosphorous in orange and other atoms coloured as they are for the helix. Despite the unravelling of upper loop, the pore and conductance remains stable.

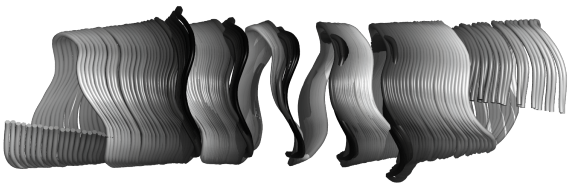

Figure 2: The unfolding β-helix shown by its backbone with the sequence colour lightening as the backbone angles are increased. The gradual increase in length, residues-per-turn, and C=O:N-H bonding is evident.

hippo/Atomix[1] it is possible to generate amino acids minimised with specified dihedral angles. Using the exact averaged value from 1GRM yielded an unstable structure that at residue counts of <60 amino acids did not fully span the membrane environment. This structure was used as a basis, and then the dihedral angles were modified by $\pm 1°$. This was repeated 40 times, with each result saved to a multi-frame .pdb file (figure 2). The overall sequence and length could then be analysed and visually examined. As the dihedrals were increased, there was only a marginal change in pore size, but the C=O:N-H distance increased, as well as the end-to-end peptide length.

The original design used GLY residues to span the hydrophobic membrane, but it became apparent that an amino acid with greater hydrophobicity was required. A GLY helix with LYS and DTRP at the ends proved to unravel and "unclick" - the crucial C=O:N-H bonds shifted and stretched, the "unclicking" being the new positioning of these constituents atoms out of step with each other. Backbone interactions along the coil of the helix were not sufficient to maintain its shape. The result was two unaligned β helices, permitting the entry of solvent into part of the bilayer, and a unstructured strand of GLY connecting to the two helices. Whilst this may prove to be sufficient to destabilise the membrane, this did not permit a continuous flow of water and ions through the membrane environment. Instead, it opened up space for a pocket of water to exist within the membrane, further unravelling the helix, but with no conductance. The original GLY designs also proved useful for providing estimates for a range of sequence lengths to cover in the next stage of the design - sequence lengths of less than 40 proved insufficient as one end of the helix was liable to obfuscation by the lipid headgroups. Conversely, sequence lengths above 60 became overly tilted and were more liable to "unclicking", as well requiring wider simulation boxes to account for their tilt, increasing calculation times.

Previous studies have elucidated the propensity of amino acid sequences (34) to sit at certain heights within the membrane. These results were used to inform the post-GLY β helix design. ALA, LEU, and VAL were all evident as being the best possible candidates for these structures. They energetically

[1]Developed and maintained by Martin and Jakob Ulmschneider, available at https://www.biowerkzeug.com/

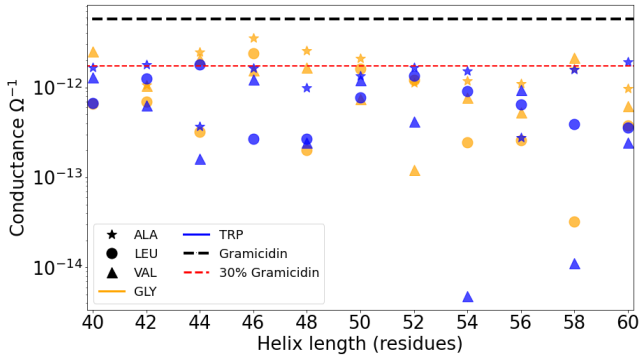

Figure 3: Conductance values for each system. The black dashed line shows the value of gramicidin's conductance as per literature, with the red dashed line showing 30% of this value. Any point on or above the red dashed line is of the same order of magnitude of gramicidin and considered a good candidate.

	Candidate name	Candidate Sequence
1	40GVG	KGKGKGKG-[Vv]$_{12}$-KGKGKGKG
2	42WAW	KwKwKwKw-[Aa]$_{13}$-KwKwKwKw
3	44GAG	KGKGKGKG-[Aa]$_{14}$-KGKGKGKG
4	44GVG	KGKGKGKG-[Vv]$_{14}$-KGKGKGKG
5	44WLW	KwKwKwKw-[Ll]$_{14}$-KwKwKwKw
6	46GAG	KGKGKGKG-[Aa]$_{15}$-KGKGKGKG
7	46GLG	KGKGKGKG-[Ll]$_{15}$-KGKGKGKG
8	48GAG	KGKGKGKG-[Aa]$_{16}$-KGKGKGKG
9	48GVG	KGKGKGKG-[Vv]$_{16}$-KGKGKGKG
10	50GAG	KGKGKGKG-[Aa]$_{17}$-KGKGKGKG
11	58GVG	KGKGKGKG-[Vv]$_{21}$-KGKGKGKG
12	60WAW	KwKwKwKw-[Aa]$_{22}$-KwKwKwKw

Table 1: Candidate systems explored in detail, with their name and full sequence. L- amino acids are shown in upper case and D- amino acids are given in lower case.

favour the centre of the hydrophobic bilayer, and are less likely to found closer to the interface (34). Their presence within the gramicidin sequence supports this as a sensible approach. To permit more favourable like-for-like comparisons, each β-helix was composed of only one species of amino acid (with both L- and D- chiralities) in its core, and with the first 8 and last 8 residues of each helix containing alternating LYS and GLY, or LYS and DTRP. It was expected that a charged amino acid like LYS would enhance head group interaction and provide a stablising effect to the structure. Indeed, previous studies have found for gramicidin mutants that using amino acids with cationic side chains in their sequence (specifically LYS) can reduce hemolytic activity whilst retaining antimicrobial potency (35).

3 RESULTS

Figure 3 shows the conductance of the 66 systems examined in this study. Ionic conductance was considered only if the ion did not recede from the direction of travel along the pore for 10 consecutive ns; in instances this criteria was not met, the ion was not considered in the calculation for conductance. Twelve of the 66 systems showed a conductance $\geq$ 30% of the gramicidin conductance. These twelve systems were then considered the candidate systems and examined in further detail - the full list of candidates in available in table 1.

There is a degree of unravelling that occurs at the membrane-solvent interface in the outer residues of the helix. This was observed in all systems, although it was more pronounced in longer sequence lengths and in systems without TRP present at the water-lipid interface. RMSD (root-mean square deviation) is a quantitative measure atomic-position similar to two structures. Thus, RMSD distributions are a good measure of how much the helix unravelled - narrower and smaller values for the peak of the distribution indicated that a helix was more prone to keeping its shape. The RMSD distributions in figure 4 are shown with solid lines for helices containing tryptophan and dashed lines for helices containing glycine. 42WAW, 44WLW and 46GAG shown the leftmost distributions and the narrowest distributions. The presence of both of the shorter conducting tryptophan helices is not a coincidence, and is a direct consequence of the role tryptophan plays in stabilising the helix through its propensity to sit at the membrane-solvent interface. Unravelling is exacerbated by the pore as water is able to enter pockets of space opened by the flexibility of the helical loop, and with the water in place these atoms are displaced and no longer available to take part in structure-stabilising backbone interactions. As interactions with the lipid headgroups decrease the helical backbone H-bond interactions, the strand loses its β-helical structure and more closely resembles a random-coil; stochastically this can lead to the charged LYS side chains blocking the entrance the pore. The residues that are enveloped by the hydrophobic environment of the lipid tails remain tightly coiled and retain their helical shape.

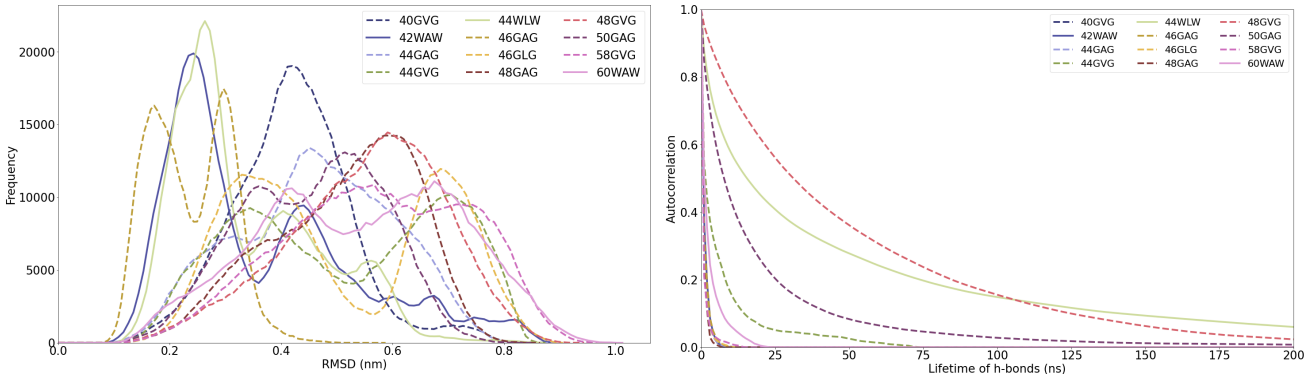

Figure 4: **Left:** Root mean square deivation (RMSD) profiles for the twelve conducting systems. The further to the left and narrower a peak is, the better the β-helix holds its shape. **Right:** Autocorrelation of the hydrogen-bond lifetimes for the twelve conducting systems. A β-helix's backbone retaining a tighter coil, and more/better C=O:N-H coupling along the backbone, can be identified by a greater area underneath the curve of the autocorrelation function.

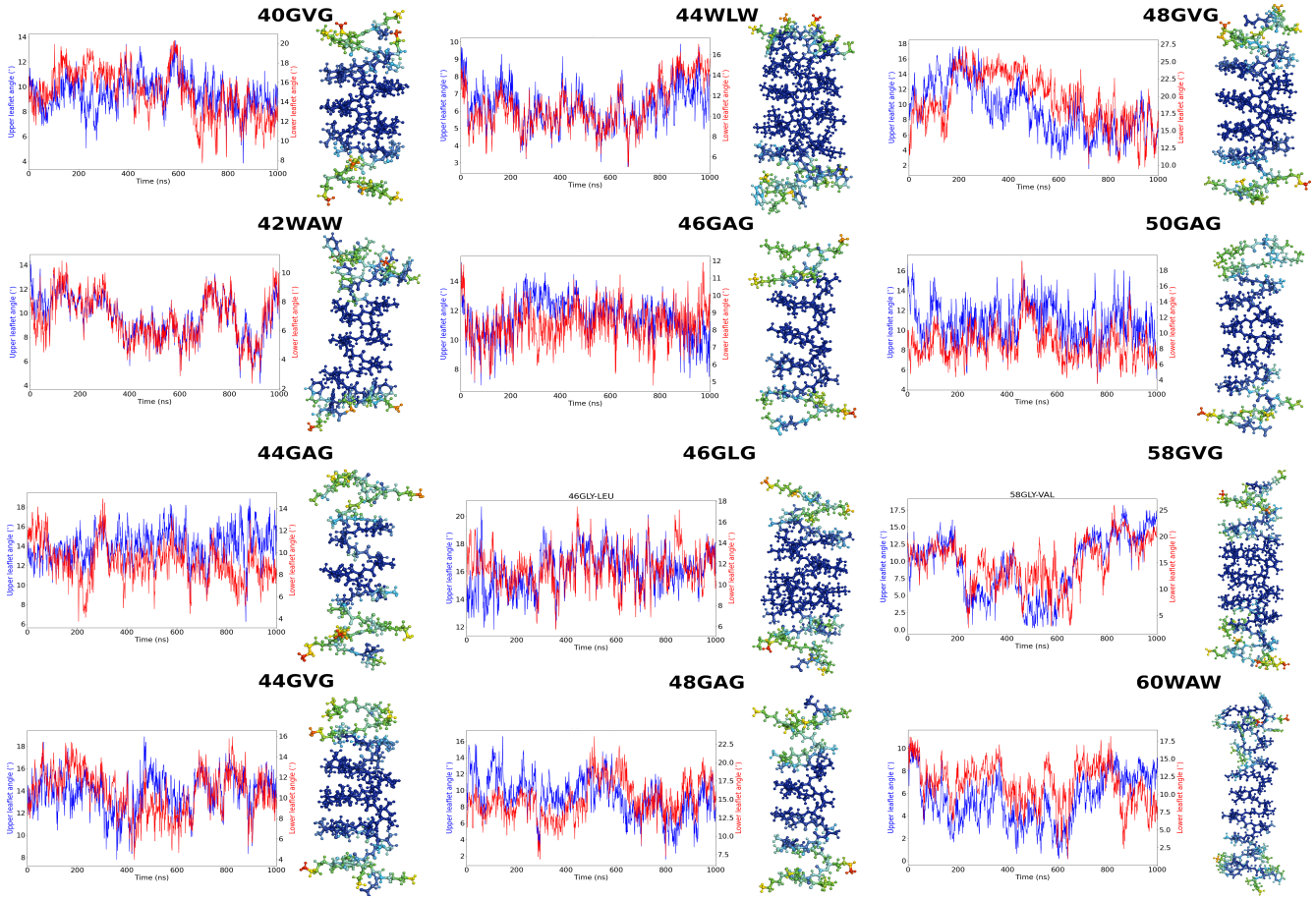

Figure 5: The angle between cntre of mass (c.o.m) of the helix and the end loops at the upper leaflet (blue) and lower leaflet (red) are shown, along with head group contact analysis for all-atoms in the helix. Head groups were considered to be anything above the glycerol unit (with tails considered to be below the glycerol unit). Atoms in blue have zero contact with these components of the lipid, and red atoms have the maximum contacts for that system. A contact was defined as being within 3.3Å.

The autocorrelation function of H-bond lifetimes (right-hand side of figure 4) reveal which sequences maintain C=O:N-H bonds along the rise of the helix. 48GVG, 44WLW, and

50GAG are the best performers by this metric. Given that 44WLW possesses a narrow RMSD it is expected that this is a relatively fixed structure, despite existing in a highly interactive environment. 20% of its hydrogen-bond interaction pairs spend at least 90ns within 3.3Å, per interaction. Many of these backbone interactions are constantly forming and reforming and thus will exist for longer than this lifetime of 90ns, with only brief interruptions in this contact.

How the helix sits within the membrane can be evaluated by considering the angles made by the ends of the helix with the centre of mass (c.o.m) of the helix itself, and the profile of interactions between helix atoms and the lipid head groups. These profiles are captured by using the contact analysis function of MDAnalysis, and colouring each atom according to the frequency at which it contacts the lipid head groups relative to other atoms in the helix (36). These figures are shown in figure 5. They are concise but a lot can be learned about these sequences from this coloured contact analysis.

It is notable that for longer sequences, it is common to find interactions with the head groups a full helical turn toward the center of the helix. In each system interactions with the headgroups are driven by LYS side chains, but the longer sequence length causes ample exposure of the beginning of the hydrophobic core of sequence to the lipid-water interface. Such an effect is less pronounced in LEU helices, a result which can be attributed to the interactions between the LEU side chains and the lipid tails. All else being equal, the hydrophobic core of VAL helices are less exposed than their ALA counterpart to the lipid headgroups, particularly at shorter sequence values. This is likely driven by the interactions between the VAL side chains and the lipid tails. With the tryptophan residues, half of the indole experiences head group interactions, whilst the other half does not. This is in agreement with what we expect from tryptophan's orientation at membrane-solvent interfaces (37) (38).

The upper and lower angles, also shown in figure 5, are the angles made the c.o.m of the loop at the upper and lower lipid-water interface residues, and the c.o.m of the full sequence. A diagramatic explanation of these angles is shown in figure 6. These angles are typically coupled for each system, following the same trajectory despite differences in their range

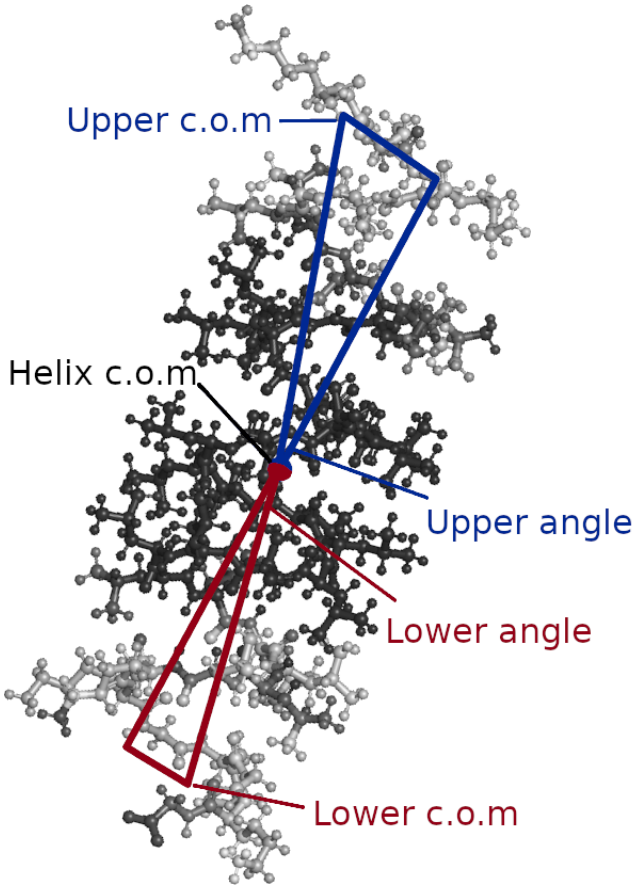

Figure 6: A diagram to demonstrate the trigonometric set up to calculate the angles made between the c.o.m of the helix and it's upper and lower extrema. These are the angles plotted in figure 5.

of values. Generally the upper leaflet angle is smaller, but this value is influenced by the unravelling typically occurring on the upper leaflet strands. Why the helical unravelling occurs only at the upper leaflet is unclear, as there is no biasing of the systems to do so and the helix is centered with the bilayer, so it should extend an equal distance above and below the center. The value for the angle by either leaflet rarely exceeds 20°. This angle influences what parts of the hydrophobic core of the helix are exposed to the head groups, with a large value exposing the hydrophobic side chains of the core to the lipid head groups.

The width of the pore is critical for the peptide's function. The HOLE program (39) (40) (41) was utilised to measure the width of the pore across the membrane at each point along the z-axis, as well as provide a measure of the stan-

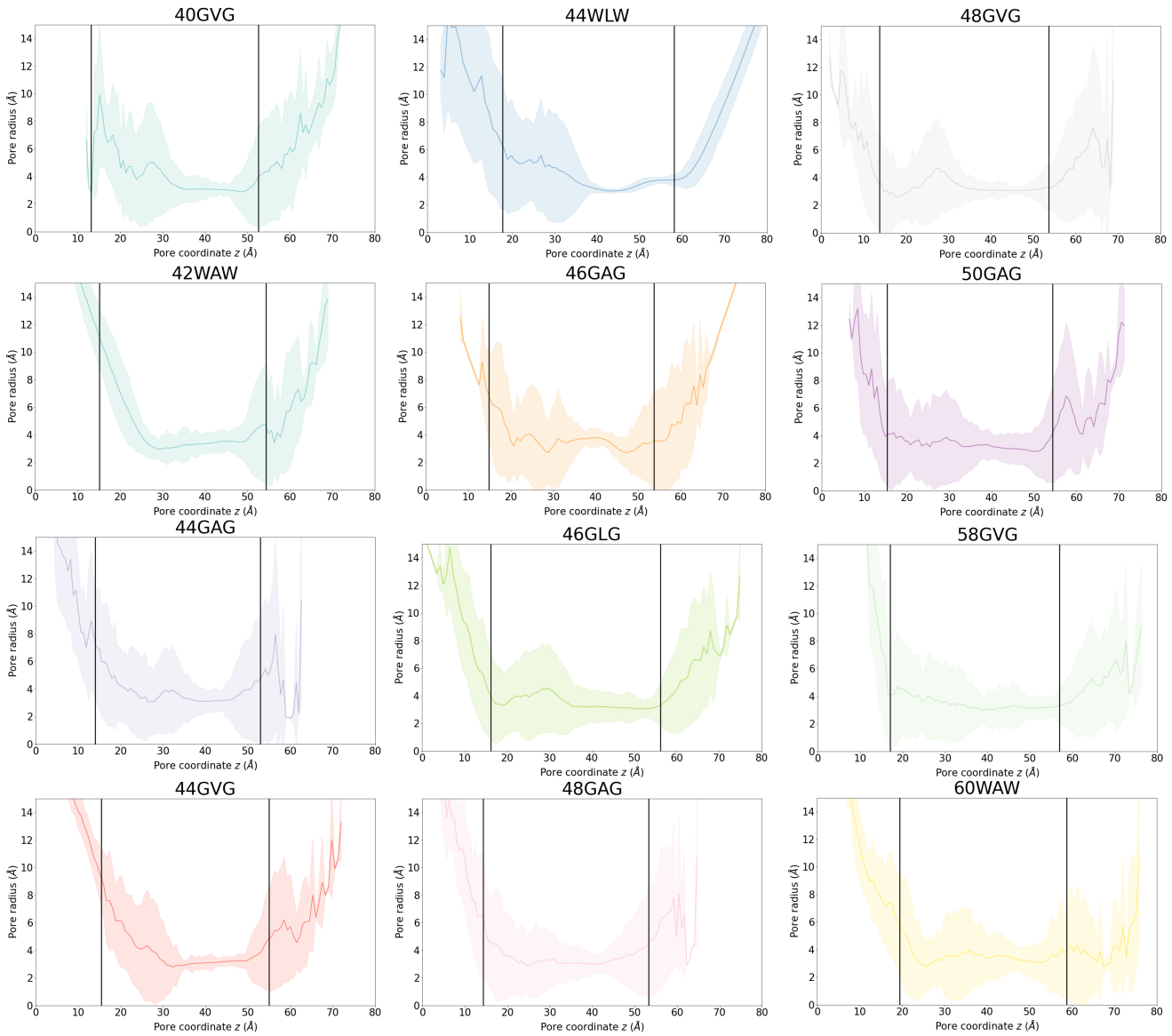

Figure 7: The pore width for each of the conducting helices, calculated using HOLE within MDAnalysis. The solid coloured line shows the mean pore width over the simulation for a given coordinate along z, and the shaded area shows the standard deviation, σ, of this mean, μ_{HOLE}. The black solid lines indicate the bounds of the membrane bilayer.

dard deviation of such a value, (see figure 7). An optimal helix will have a very small standard deviation at every point within the membrane, demarcated by the black lines. The two shorter tryptophan distributions (42WAW and 44WLW) show at certain points neglible σ values which reveals a remarkably stable structure at that section of the membrane, with little to no movement. This behaviour is lost for the longer 60WAW tryptophan helix, suggesting there exists an optimal sequence length between 42 and 60 amino acids. It is generally true for the GLY capped helices too, that longer sequences showed a greater deviation in their width. For the shorter helices, deviations within the bounds of the membrane are explained by the loss of structure of the end helical loop and the breaking of hydrogen-bond interactions as a result of this, leading to a wider structure with less positional rigidity.

4 CONCLUSION

These β-helical peptides show promise as candidate peptides for antimicrobial peptides in Gram-positive lipid membranes. There are several avenues to pursue for improvements to such peptides; one such approach would be to use non-homogeneous protein sequences - LEU made up only two of the 12 candidate systems, but 44WLW showed the most pore stability. Given that ALA made up six of the 12 candidates, but showed the greatest deviation in pore width, combining LEU and ALA at the appropriate points along the amino acid sequence may result in a helix that offers a consistent width and can efficiently conduct ions. More residues per turn would afford a wider pore, although a higher sequence length would make synthesis for future in vivo testing more challenging. However this wider pore would also allow more than just water and ions to passage through the pore, and could potentially be a way to allow select small molecules into the cell, which would be a fine result. Another direction would be attached lipids at the N and C termini of the helix to offer stability. This last method may also result in greater binding affinity to membranes, and can help fine tune the selectivity of the helix for particular membrane compositions through the choice of attached lipid.

5 AUTHOR CONTRIBUTIONS

MBU designed the research. EL generated the structures, performed the analysis, and wrote the article. MBU reviewed the article.

6 ACKNOWLEDGMENTS

This work was done with funding from EPSRC via the Cross-disciplinary Approaches to Non-Equilibrium Systems (CANES) CDT and the BBSRC. Simulations were carried out on the GRAVITY and CREATE supercomputing infrastructure at King's College London. The authors have no relevant financial ties to disclose. The authors thank Dr. Dominique Hoogland for her sage advice and her help in reviewing the article.

REFERENCES

1. Andersen, O. S., 1984. Gramicidin Channels. *Annual Review of Physiology* 46:531–548. https://doi.org/10.1146/annurev.ph.46.030184.002531.

2. Gause, G. F., and M. G. Brazhnikova, 1944. Gramicidin S and its use in the treatment of infected wounds. *Nature* 154:703–703.

3. Dubos, R. J., 1939. Studies on a bactericidal agent extracted from a soil bacillus. *Journal of Experimental Medicine* 70:1–10. https://doi.org/10.1084/jem.70.1.1.

4. Sarges, R., and B. Witkop, 1965. Gramicidin A. V. The Structure of Valine- and Isoleucine-gramicidin A. *Journal of the American Chemical Society* 87:2011–2020. https://doi.org/10.1021/ja01087a027.

5. Kelkar, D. A., and A. Chattopadhyay, 2007. The gramicidin ion channel: A model membrane protein. *Biochimica et Biophysica Acta (BBA) - Biomembranes* 1768:2011–2025. https://doi.org/10.1016/j.bbamem.2007.05.011.

6. Wallace, B., 1998. Recent Advances in the High Resolution Structures of Bacterial Channels: Gramicidin A. *Journal of Structural Biology* 121:123–141. https://doi.org/10.1006/jsbi.1997.3948.

7. Veatch, W., and L. Stryer, 1977. The dimeric nature of the gramicidin A transmembrane channel: Conductance and fluorescence energy transfer studies of hybrid channels. *Journal of Molecular Biology* 113:89–102. https://doi.org/10.1016/0022-2836(77)90042-0.

8. Mueller, P., D. O. Rudin, H. T. Tien, and W. C. Wescott, 1963. Methods for the formation of single bimolecular lipid membranes in aqueous solution. *The journal of physical chemistry* 67:534–535.

9. Hladky, S., and D. Haydon, 1972. Ion transfer across lipid membranes in the presence of gramicidin A. *Biochimica et Biophysica Acta (BBA) - Biomembranes* 274:294–312. https://doi.org/10.1016/0005-2736(72)90178-2.

10. Wallace, B. A., 1990. Gramicidin Channels and Pores. *Annual Review of Biophysics and Biophysical Chemistry* 19:127–157. https://doi.org/10.1146/annurev.bb.19.060190.001015.

11. de Jesus, A. J., and T. W. Allen, 2013. The role of tryptophan side chains in membrane protein anchoring and hydrophobic mismatch. *Biochimica et Biophysica Acta (BBA) - Biomembranes* 1828:864–876. https://doi.org/10.1016/j.bbamem.2012.09.009.

12. Andersen, O., R. Koeppe, and B. Roux, 2005. Gramicidin Channels. *IEEE Transactions on Nanobioscience* 4:10–20. https://doi.org/10.1109/tnb.2004.842470.

13. Killian, J. A., 1992. Gramicidin and gramicidin-lipid interactions. *Biochimica et Biophysica Acta (BBA) - Reviews on Biomembranes* 1113:391–425. https://doi.org/10.1016/0304-4157(92)90008-x.

14. O'Connell, A. M., R. E. Koeppe, and O. S. Andersen, 1990. Kinetics of Gramicidin Channel Formation in Lipid Bilayers: Transmembrane Monomer Association. *Science* 250:1256–1259. https://doi.org/10.1126/science.1700867.

15. Jenkins, J., O. Mayans, and R. Pickersgill, 1998. Structure and Evolution of Parallel -Helix Proteins. *Journal of Structural Biology* 122:236–246. https://www.sciencedirect.com/science/article/pii/S1047847798939855.

16. David, J. M., and A. K. Rajasekaran, 2015. Gramicidin A: A New Mission for an Old Antibiotic. *Journal of Kidney Cancer and VHL* 2:15–24. https://doi.org/10.15586/jkcvhl.2015.21.

17. Wallace, B., and K. Ravikumar, 1988. The gramicidin pore: crystal structure of a cesium complex. *Science* 241:182–187.

18. Jenkins, J., O. Mayans, and R. Pickersgill, 1998. Structure and Evolution of Parallel β-Helix Proteins. *Journal of Structural Biology* 122:236–246. https://doi.org/10.1006/jsbi.1998.3985.

19. Yoder, M. D., and F. Jurnak, 1995. The parallel iβ/i helix and other coiled folds. *The FASEB Journal* 9:335–342. https://doi.org/10.1096/fasebj.9.5.7896002.

20. Cowen, L., P. Bradley, M. Menke, J. King, and B. Berger, 2002. Predicting the Beta-Helix Fold from Protein Sequence Data. *Journal of Computational Biology* 9:261–276. https://doi.org/10.1089/10665270252935458.

21. Huang, J., S. Rauscher, G. Nawrocki, T. Ran, M. Feig, B. L. De Groot, H. Grubmüller, and A. D. MacKerell Jr, 2017. CHARMM36m: an improved force field for folded and intrinsically disordered proteins. *Nature methods* 14:71–73.

22. Spoel, D. V. D., E. Lindahl, B. Hess, G. Groenhof, A. E. Mark, and H. J. C. Berendsen, 2005. GROMACS: Fast, flexible, and free. *Journal of Computational Chemistry* 26:1701–1718. https://doi.org/10.1002/jcc.20291.

23. Abraham, M. J., T. Murtola, R. Schulz, S. Páll, J. C. Smith, B. Hess, and E. Lindahl, 2015. GROMACS: High performance molecular simulations through multi-level parallelism from laptops to supercomputers. *SoftwareX* 1-2:19–25. https://doi.org/10.1016/j.softx.2015.06.001.

24. Malanovic, N., and K. Lohner, 2016. Antimicrobial Peptides Targeting Gram-Positive Bacteria. *Pharmaceuticals* 9:59. https://doi.org/10.3390/ph9030059.

25. Darden, T., D. York, and L. Pedersen, 1993 98:10089–10092. https://doi.org/10.1063/1.464397.

26. Berendsen, H. J. C., J. P. M. Postma, W. F. van Gunsteren, A. DiNola, and J. R. Haak, 1984. Molecular dynamics with coupling to an external bath. *The Journal of Chemical Physics* 81:3684–3690. https://doi.org/10.1063%2F1.448118.

27. Evans, D. J., and B. L. Holian, 1985. The nose–hoover thermostat. *The Journal of chemical physics* 83:4069–4074.

28. Nosé, S., and M. Klein, 1983. Constant pressure molecular dynamics for molecular systems. *Molecular Physics* 50:1055–1076. https://doi.org/10.1080/00268978300102851.

29. Humphrey, W., A. Dalke, and K. Schulten, 1996. VMD: visual molecular dynamics. *Journal of molecular graphics* 14:33–38.

30. Michaud-Agrawal, N., E. J. Denning, T. B. Woolf, and O. Beckstein, 2011. MDAnalysis: A toolkit for the analysis of molecular dynamics simulations. *Journal of Computational Chemistry* 32:2319–2327. https://doi.org/10.1002/jcc.21787.

31. Smith, P., and C. D. Lorenz, 2021. LiPyphilic: A Python Toolkit for the Analysis of Lipid Membrane Simulations. *Journal of Chemical Theory and Computation* 17:5907–5919. https://doi.org/10.1021/acs.jctc.1c00447.

32. DeLano, W. L., et al., 2002. Pymol: An open-source molecular graphics tool. *CCP4 Newsl. Protein Crystallogr* 40:82–92.

33. Arseniev, A., I. Barsukov, A. Lomize, V. Orekhov, and V. Bystrov, 1994. Refinement of the spatial structure of the Gramicidin A transmembrane Ion channel. https://doi.org/10.2210/pdb1grm/pdb.

34. Ulmschneider, M. B., and M. S. Sansom, 2001. Amino acid distributions in integral membrane protein structures. *Biochimica et Biophysica Acta (BBA) - Biomembranes* 1512:1–14. https://doi.org/10.1016/s0005-2736(01)00299-1.

35. Zerfas, B. L., Y. Joo, and J. Gao, 2016. Gramicidin A Mutants with Antibiotic Activity against Both Gram-Positive and Gram-Negative Bacteria. *ChemMedChem* 11:629–636. https://doi.org/10.1002/cmdc.201500602.

36. Waller, C., J. K. Marzinek, E. McBurnie, P. J. Bond, P. T. Williamson, and S. Khalid, 2023. Impact on S. aureus and E. coli membranes of treatment with chlorhexidine and alcohol solutions: insights from molecular simulations and nuclear magnetic resonance. *Journal of Molecular Biology* 435:167953.

37. Esbjörner, E. K., C. E. Caesar, B. Albinsson, P. Lincoln, and B. Nordén, 2007. Tryptophan orientation in model lipid membranes. *Biochemical and biophysical research communications* 361:645–650.

38. van der Wel, P. C., N. D. Reed, D. V. Greathouse, and R. E. Koeppe, 2007. Orientation and motion of tryptophan interfacial anchors in membrane-spanning peptides. *Biochemistry* 46:7514–7524.

39. Smart, O., J. Goodfellow, and B. Wallace, 1993. The pore dimensions of gramicidin A. *Biophysical Journal* 65:2455–2460. https://doi.org/10.1016/s0006-3495(93)81293-1.

40. Smart, O. S., J. G. Neduvelil, X. Wang, B. Wallace, and M. S. Sansom, 1996. HOLE: A program for the analysis of the pore dimensions of ion channel structural models. *Journal of Molecular Graphics* 14:354–360. https://doi.org/10.1016/s0263-7855(97)00009-x.

41. Stelzl, L. S., P. W. Fowler, M. S. Sansom, and O. Beckstein, 2014. Flexible Gates Generate Occluded Intermediates in the Transport Cycle of LacY. *Journal of Molecular Biology* 426:735–751. https://doi.org/10.1016/j.jmb.2013.10.024.

SUPPLEMENTARY MATERIAL

Made available on the lead author's github.